Floating phase in a 2D ANNNI model



2007 J. Phys. A: Math. Theor. 40 6251

(http://iopscience.iop.org/1751-8121/40/24/001)

J. Phys. A: Math. Theor. **40** (2007) 6251–6265 doi:10.1088/1751-8113/40/24/001

# Floating phase in a 2D ANNNI model

**Anjan Kumar Chandra and Subinay Dasgupta**

Department of Physics, University of Calcutta, 92 Acharya Prafulla Chandra Road, Calcutta 700 009, India

Received 16 February 2007, in final form 18 April 2007
Published 30 May 2007
Online at stacks.iop.org/JPhysA/40/6251

**Abstract**

We investigate whether the floating phase (where the correlation length is infinite and the spin–spin correlation decays algebraically with distance) exists in the temperature ($T$)—frustration parameter ($\kappa$) phase diagram of 2D ANNNI model. To identify this phase, we look for the region where (i) finite size effect is prominent and (ii) some relevant physical quantity changes somewhat sharply and this change becomes sharper as the system size increases. For $\kappa < 0.5$, the low-temperature phase is ferromagnetic and we study energy and magnetization. For $\kappa > 0.5$, the low-temperature phase is antiphase and we study energy, layer magnetization, length of domain walls running along the direction of frustration, number of domain-intercepts that are of length 2 along the direction of frustration, and the number of domain walls that do not touch the upper and/or lower boundary. In agreement with some previous studies, our final conclusion is that the floating phase exists, if at all, only along a line.

PACS numbers: 05.70.Jk, 05.10.Ln, 64.60.Fr

## 1. Introduction

The two-dimensional axial next-nearest-neighbour Ising (ANNNI) model $\left(\text{spin} = \frac{1}{2}\right)$ is a square lattice Ising model with nearest-neighbour ferromagnetic interaction along both the axial directions and second-neighbour anti-ferromagnetic interaction along one axial direction. The Hamiltonian is

$$\mathcal{H} = -J \sum_{x,y} s_{x,y}[s_{x+1,y} + s_{x,y+1} - \kappa s_{x+2,y}] \tag{1}$$

where the sites $(x, y)$ run over a square lattice, the spins $s_{x,y}$ are $\pm 1$, $J$ is the nearest-neighbour interaction strength and $\kappa$ is a parameter of the model. For positive values of $\kappa$, the second-neighbour interaction introduces a frustration. This is one of the simplest frustrated classical Ising models with a tunable frustration and has been studied over a long time ([1–3] for review). The most widely studied aspect of this model is the phase diagram in the $T - \kappa$ phase space, where $T$ stands for temperature. It is easy to prove analytically that [1–3] at zero temperature,

  

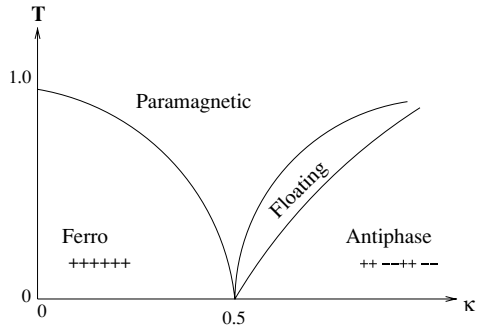


**Figure 1.** Schematic phase diagram of the two-dimensional ANNNI model according to previous studies.

the system is in a ferromagnetic state for $\kappa < 0.5$, and in antiphase ($++--++--\cdots$ along the $x$ direction and all like spins along the $y$ direction) for $\kappa > 0.5$ with a 'multiphase' state at $\kappa = 0.5$. (The multiphase state comprises all possible configurations that have no domain of length 1 along the $x$ direction.)

From Monte Carlo simulations and approximate analytic calculations, some early studies had proposed a phase diagram (figure 1) consisting of a ferromagnetic phase (for $\kappa < 0.5$) and antiphase (for $\kappa > 0.5$) at low temperature along with a paramagnetic phase at high temperature (for all $\kappa$ values). The crucial point is, between the ordered and the disordered phases for $\kappa > 0.5$, there may be a so-called floating phase characterized by (i) a spin–spin correlation that decays algebraically with distance and (ii) an incommensurate, continuously varying modulation. An approximate analytic treatment by Villain and Bak [4] predicted that (for $\kappa > 0.5$) as temperature increases from zero, there is a second-order Pokrovsky–Talapov-type commensurate-incommensurate phase transition from antiphase to the floating phase followed by a Kosterlitz–Thouless transition from the floating to the paramagnetic phase. This leads to a phase diagram shown schematically in figure 1. Several computational studies (see [1, 5]) also confirmed such a phase diagram. Later, Shirahata and Nakamura [5] have measured the dynamical exponent by studying the non-equilibrium relaxation of order parameter at $\kappa = 0.6$ and 0.8 and concluded that the floating phase exists, if at all, over a narrow temperature range only. The central problem in this study is that the identification of order parameter is ambiguous for $\kappa > 0.5$, in the sense that it is difficult to identify a physical observable that relaxes algebraically at the critical temperature. One may note that the antiphase magnetization

$$M_{\langle 2\rangle} = \sum_{x,y} s^{\langle 2\rangle}_{x,y} s_{x,y}$$

does not satisfy this criterion [5]. (Here, $s^{\langle 2\rangle}_{x,y}$ is the spin distribution for perfect aniphase distribution.) Recently, a density matrix renormalization group analysis [6] has also excluded the presence of any incommensurate phase over an extended region.

The 2D ANNNI model is related to the transverse ANNNI chain by Suzuki–Trotter transformation [7–10]. This quantum Ising model has also been studied widely. Numerical and approximate analytic studies [9, 11, 12] had predicted that the floating phase exists in the transverse ANNNI chain over a region, as shown in figure 1. However, recently we have shown [13] that for this model, the floating phase exists over a wide region extending from $\kappa < 0.5$ to $\kappa > 0.5$. There is thus a controversy about the existence of algebraically decaying phase in the 2D ANNNI model.

In this paper, we shall present Monte Carlo simulation of the 2D ANNNI model with a view to locating the floating phase, if any. For $\kappa < 0.5$, one can easily identify the magnetization as the order parameter and for this case we have therefore measured

(1) internal energy,
(2) magnetization.

For $\kappa > 0.5$, the ordered phase is 'antiphase' and it is difficult to identify the order parameter unambiguously. In this case, we have measured

(1) internal energy,
(2) layer magnetization (magnetization perpendicular to the direction of frustration),
(3) length of domain walls running along the direction of frustration,
(4) number of domain-intercepts that are of length 2 over a straight line along the direction of frustration,
(5) number of dislocations measured as the number of domain walls that do not touch the upper and/or lower boundary.

We shall discuss later (section 3) the significance of these quantities in the context of our work.

From the measurement of a suitable physical quantity $Q(t)$ at a time $t$, the critical point (or, for that matter, the critical region) could be identified from the general principle that at the critical point the quantity $Q(t) - Q(\infty)$ is expected to vanish algebraically as a function of time $t$. While this characteristic is handy for the case $Q(\infty) = 0$, it is not usable when $Q(\infty) \neq 0$, as very large time simulation is required to measure the quantity $Q(\infty)$ itself. In such cases, we have utilized two essential features of critical phenomena: (i) for a finite lattice, the correlation time will diverge as [14]

$$\tau \sim L^z.$$

Hence, the quantity $Q(t)$ will depend strongly on the system size only at the critical temperature $T_c$ even at finite values of $t$. (ii) the equilibrium value $Q(\infty)$ will undergo a sudden change, which is detectable even for small size and becomes more and more drastic as the system size increases.

As mentioned above, the results from non-equilibrium relaxation study [5] and the density matrix renormalization group analysis [6] contradicts the previous studies [5, 9, 15] as regards the extent of the floating phase. This paper confirms the conclusion of the former two studies by Monte Carlo simulation. One should note that all these studies agree at sufficiently low temperatures. We measure some observables that play a crucial role in the underlying physics and that have not been analysed till now.

In sections 2 and 3, we shall present the simulation studies for $\kappa < 0.5$ and $\kappa > 0.5$ respectively. All the simulation studies were performed with sequential Metropolis algorithm using periodic boundary conditions in the $X$ and $Y$ directions and the results were averaged over 10 to 50 realizations. In section 4, we shall study the correspondence between the 2D ANNNI model and the transverse ANNNI chain and in section 5 present conclusions. Our final conclusion is that the divergent correlation time exists only along a line. The phase diagram obtained is presented in figure 2. Everywhere in this communication temperature is measured in unit of $T_c^{(0)} = 0.44069$, the critical temperature for nearest-neighbour interaction ($\kappa = 0$). This diagram is in qualitative agreement with that obtained by Shirahata and Nakamura [5] and Derian, Gendiar and Nishino [6]. The small difference between our results and those obtained by these authors seems to be due to the small ($\sim 1000 \times 1000$) size of our simulation, compared to that of Shirahata and Nakamura ($\sim 6399 \times 6400$).

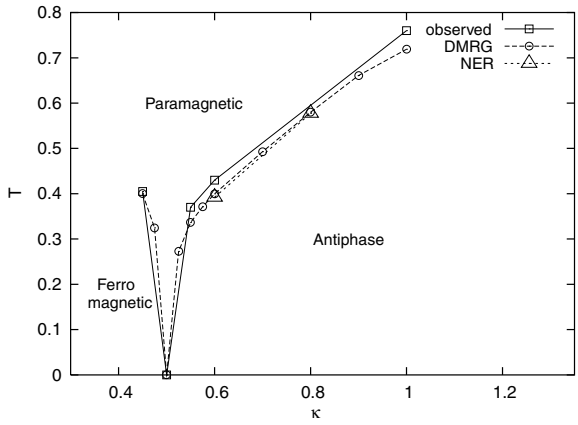


**Figure 2.** The phase diagram of the two-dimensional ANNNI model as obtained from the present study, from nonlinear relaxation (NER) [5] and density matrix renormalization group (DMRG) [6]. The temperature is measured in units of $T_c^{(0)} = 0.44069$ as mentioned in the text.

## 2. Simulation studies for $\kappa < 0.5$

### *2.1. Energy*

Before we consider the measurements on the 2D ANNNI model itself, let us break off for a discussion on critical behaviour of energy relaxation in general. Internal energy $E$ is always unambiguously defined, in contrast to the order parameter, which for some phase transitions (like our system for $\kappa > 0.5$) may not be easy to identify and measure. However, since $E(\infty) \neq 0$, it is difficult to study the time variation of the quantity $E(t) - E(\infty)$, as mentioned above. The relaxation of energy has also been studied elsewhere [16, 17].

We shall now consider the case of $\kappa = 0$ (only nearest-neighbour interaction), and obtain the exponent, following standard scaling arguments [16, 18, 19]. Starting from the standard diffusion equation for the (non-conserved) order parameter $\psi$

$$\frac{\partial \psi}{\partial t} = -\Gamma \frac{\partial F}{\partial \psi}$$

one obtains

$$\frac{\partial F}{\partial t} = -\frac{1}{\Gamma}\left(\frac{\partial \psi}{\partial t}\right)^2,$$

where $F$ is the appropriate free energy and $\Gamma$ is a parameter of the model. The identity $E = \partial(\beta F)/\partial\beta$, where $E$ is the total internal energy then gives

$$\frac{\partial E}{\partial t} = -\frac{1}{\Gamma}\left(1 + \beta\frac{\partial}{\partial \beta}\right)\left(\frac{\partial \psi}{\partial t}\right)^2. \tag{2}$$

The scaling relation for the order parameter may be written as [19],

$$\psi(t, \epsilon, L, \psi_0) = b^{-\beta/\nu}\psi(b^{-z}t, b^{1/\nu}\epsilon, b^{-1}L) \tag{3}$$

where $\epsilon = (1-T)$ ($T$ being the temperature measured in units of $T_c^{(0)}$), $L$ is the linear dimension of the system, $b$ is the scaling factor, and $\psi_0$ is the initial value of the order parameter. Also, $\beta$ and $\nu$ are the static critical exponents, and $z$ is the dynamic critical exponent. Choosing $b = t^{1/z}$ and suppressing the unimportant arguments $L$ ($\to\infty$) and $\psi_0$, we obtain

$$\psi(t, \epsilon) = t^{-\beta/\nu z}[\psi(1, 0) + t^{1/\nu z}\epsilon\psi'(1, 0)] \tag{4}$$

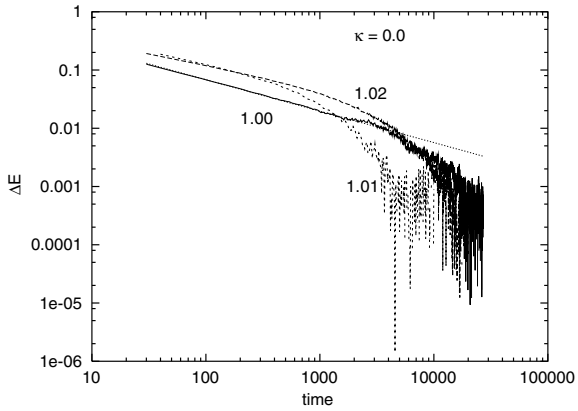


**Figure 3.** Energy relaxation for a $1000 \times 1000$ lattice for only nearest-neighbour interaction i.e. $\kappa = 0$, starting from an ordered (all up) configuration. The straight line is a guide to the eye and fits to $0.82t^{-0.54}$.

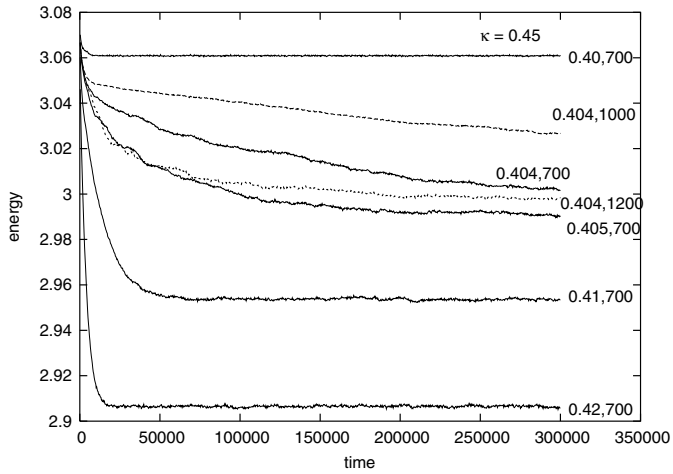


**Figure 4.** Energy relaxation for $\kappa = 0.45$ at temperature $T$ for $L \times L$ square lattice. The numbers at the right margin indicate $T$ and $L$ values. It is important to note that for $T = 0.40$, 0.405, 0.41 and 0.42, the curves for $L = 1000$ and 1200 coincide with that of $L = 700$.

where $\psi'$ is the derivative of $\psi$ with respect to $\epsilon$. Substituting this form in equation (2), we have, for large time,

$$\Delta E \sim t^{-\sigma} \tag{5}$$

where $\Delta E$ is the energy difference $E(t) - E(\infty)$ and $\sigma = 1 - (1 - 2\beta)/\nu z = 0.66$. Our simulations confirm this value of sigma (figure 3).

In the case of the ANNNI model ($\kappa$ nonzero but $< 0.5$) we study the energy relaxation starting from ferromagnetic state. Our results for $\kappa = 0.45$ is as follows. The $E(t)$ versus $t$ curve for an $L \times L$ lattice is the same for $L = 700$, 1000 and 1200 at a temperature $T = 0.40$ (in units of $T_c^{(0)}$). This happens also for $T = 0.41$ but not for $T = 0.404$, where the relaxation behaviour depends on $L$ to the largest extent (figure 4). At $L = 700$, we could evaluate $E(\infty)$ and found that $E(t) - E(\infty)$ versus $t$ plot shows an algebraic decay around $T = 0.40$

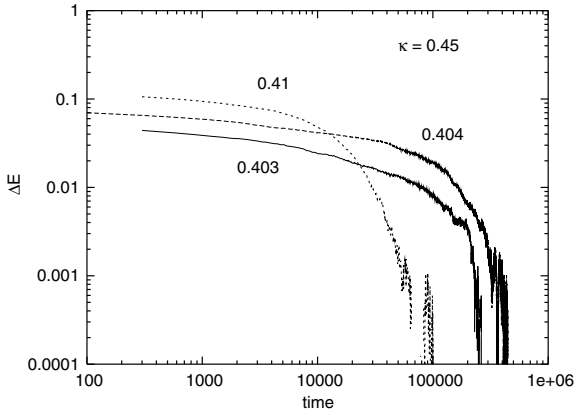


**Figure 5.** Energy relaxation for $\kappa = 0.45$ for $700 \times 700$ lattice. The numbers indicate temperature. Note that the linear (algebraic) region is most prominent for $T = 0.404$. The algebraic region fits to $0.17t^{-0.15}$. We could not furnish the curve for $T = 0.405$ as the system takes too long time to equilibrate.

but the algebraic region is most extended for $T = 0.404$ (figure 5). It is hence concluded that at $\kappa = 0.45$, the critical point is $T_c = 0.404 \pm 0.002$. We could not however evaluate $E(\infty)$ for $L = 1000$ or 1200 as they involve too much computational time. Moreover, even at $T = 0.404$, there is some anomaly in the sense that the decay of $E(t)$ at $L = 1200$ is *faster* (rather than slower) than that for $L = 700$ and 1000 (figure 4). A simulation over a longer time scale might resolve the anomaly.

It is interesting to note that at $\kappa = 0.45, T = 0.404$, the exponent $\sigma$ has a value $0.15 \pm 0.05$. Although it is a computationally intensive job to determine $\sigma$ accurately, we attempted to study the apparent variation of $\sigma$ with $\kappa$ and found that it does not change much till $\kappa = 0.4$ and afterwards decrease markedly.

### *2.2. Magnetization*

For $\kappa < 0.5$, the order parameter is magnetization $M$, whose equilibrium value is zero at the critical point. Hence, an easy method of locating the critical point is to investigate where the magnetization relaxes algebraically. It is well-known (equation (4)) that at $T_c$ the magnetization decays as

$$M \sim t^{-\sigma'} \tag{6}$$

where $\sigma' = \beta/\nu z$. For $\kappa = 0$, the value of $\sigma'$ is 0.057 34.

At $\kappa = 0.45$ the magnetization is found to relax algebraically only around $T = 0.405 \pm 0.002$, which therefore is the critical temperature (figure 6). That the critical temperature at $\kappa = 0.45$ lies between 0.40 and 0.41 is also verified by the fact that there is a sudden change in the equilibrium value of magnetization as temperature increases from 0.40 to 0.41, and that this change becomes more and more sudden as the lattice size increases (figure 7).

The exponent for magnetization decay turns out to be $\sigma' = 0.02 \pm 0.005$ at $\kappa = 0.45$, $T = 0.404$. As for the case of energy relaxation, it is a computationally intensive job to determine $\sigma'$ accurately. Approximate measurements indicate that just like $\sigma$, the exponent $\sigma'$ also remains more or less the same up to $\kappa = 0.4$ and starts decreasing markedly at higher $\kappa$. Further investigations on the apparent variation of $\sigma$ and $\sigma'$ is in progress.

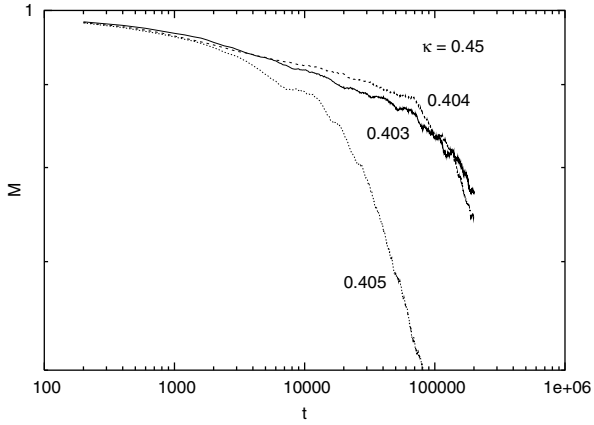


**Figure 6.** Relaxation of magnetization at $\kappa = 0.45$ for $1000 \times 1000$ lattice. The linear (algebraic) region is most prominent for $T = 0.404$ and fits to $1.08t^{-0.017}$.

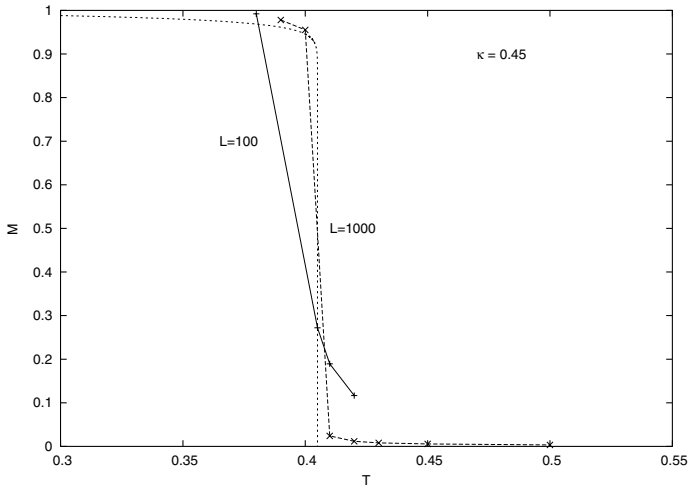


**Figure 7.** Equilibrium value of magnetization at $\kappa = 0.45$ as a function of temperature.

## 3. Simulation studies for $\kappa > 0.5$

In this case, it is difficult to identify the order parameter, as mentioned above. It can be easily proved [1–3] that, at low temperature the system is in a perfectly ordered state with like spins along the $Y$ axis and $++--$ pattern repeated along the $X$ direction. The domain walls thus run exactly parallel to the $Y$ axis. Moving along the $X(Y)$ axis, one finds domains of length 2 ($L$), for an $L \times L$ system. As one increases the temperature, after some temperature $T_c$ (called the lower critical temperature), domains of length larger than 2 appear along the $X$ direction. The domain walls now run not always parallel to the $Y$ axis. They start from the lower boundary and terminate at the upper, but they often take small steps parallel to the $X$ axis. Along the $Y$ axis the domains are now sometimes less than $L$ in length. Villain and Bak [4] pointed out that the number of domains that do not touch *both* boundaries is crucial and

represents some sort of 'dislocation'. This number is almost zero immediately above $T_c$ but suddenly increases at some temperature $T_2$. While $T_c$ marks a second-order commensurate–incommensurate (Pokrovsky–Talapov type) transition, $T_2$ marks a Kosterlitz–Thouless type transition. For $T > T_2$ domains of small size appear in the $X$ and $Y$ direction and the system is in a paramagnetic state. For $T_c < T < T_2$, Villain and Bak claimed that, the wavelength of modulation changes continuously with temperature and the correlation length is infinity, leading to a spin–spin correlation that decays algebraically with distance.

To study the two transitions, one at $T = T_c$ and the other at $T = T_2$, we measure several quantities always starting the simulation with antiphase as the initial configuration.

(1) Internal energy is studied in the same way as done for $\kappa < 0.5$.

(2) Layer magnetization is defined (following [5]) as the magnetization of a chain along the $Y$ axis averaged over all such chains:

$$m_l = \frac{1}{L}\sum_{x=1}^{L} |m_x| \tag{7}$$

where

$$m_x = \frac{1}{L}\sum_{y=1}^{L} s_{x,y}.$$

Obviously, this quantity should be 1 for $T < T_c$ and zero above $T_2$. Hence, the size dependence of the relaxation of $m_l$ and the algebraic nature of relaxation of $m_l$ would indicate a diverging correlation length. Shirahata and Nakamura [5] have studied this quantity to identify the upper transition temperature $T_2$ at $\kappa = 0.60$ and 0.80.

(3) The sum of length of the segments of domain walls that are parallel to the $X$ axis, divided by the system size gives a quantity (say, $d_x$) which is strictly zero in the perfect antiphase, but increases suddenly to some nonzero value at $T_c$. Its measurement leads to an estimate of $T_c$.

(4) Moving in the $X$ direction, one may note the lengths of domain intercepts encountered, and compute the ratio

$$f_2 = n_2/n_t$$

where $n_2$ is the number of domains of length 2 and $n_t$ is the total number of domains. This ratio is 1 for $T < T_c$ and decreases for higher $T$. We note the region over which the relaxation of $f_2$ depends on size or is algebraic in nature.

(5) The spin domains are identified and the fraction ($f_d$) of domains that do not touch the upper and/or lower boundary is counted. (Those which miss any one boundary is counted with weightage 1 and those which miss both the boundaries are given weightage 2.) This fraction measures the number of 'dislocations' that drives the Kosterlitz–Thouless phase transition at $T_2$. We do not study the relaxation of this quantity for computational limitations, but obtain from simulation the equilibrium value away from $T_c$. Such measurement should lead to an estimation of the Kosterlitz–Thouless transition temperature $T_2$, if any.

The study of all these quantities leads us to the conclusion that the floating phase, i.e. the region between $T_c$ and $T_2$ extends, if at all, over a temperature range less than 0.02. Thus, the region of diverging correlation length exists *only along a line*, up to the accuracy of this study. Our study was performed at $\kappa = 0.55$, 0.60, 1.0. The resulting phase diagram is presented in figure 2. However, it is interesting to observe that while the width of the critical region is 0.02 for $\kappa > 0.5$, it is much less, about 0.001, for $\kappa < 0.5$.

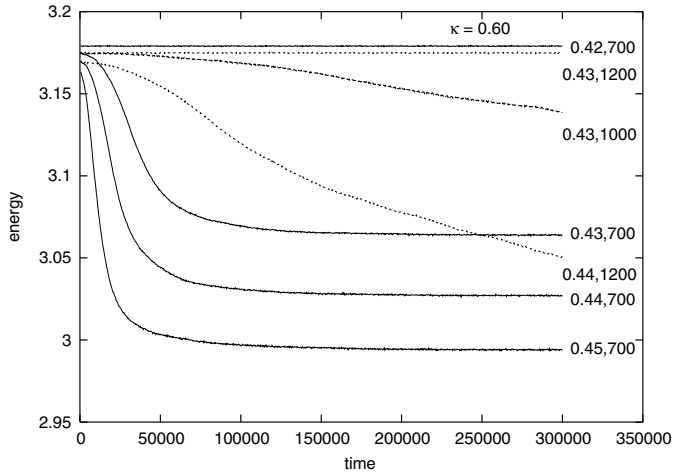


**Figure 8.** Energy relaxation for $\kappa = 0.60$ at temperature $T$ for $L \times L$ square lattice. The numbers at the right margin indicate $T$ and $L$ values. For $T = 0.42$ and 0.45, the curves for $L = 1000$ and 1200 coincide with that of $L = 700$.

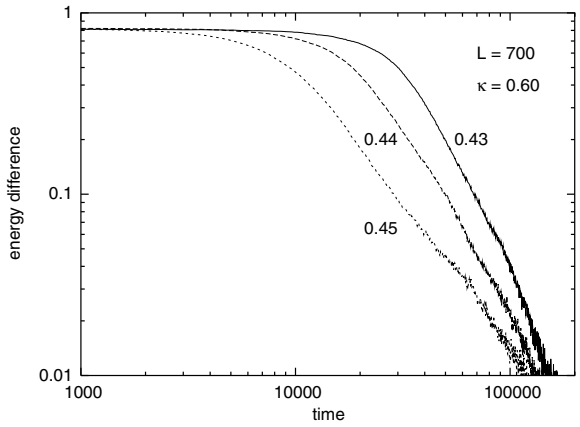


**Figure 9.** Energy relaxation for $\kappa = 0.60$ for $700 \times 700$ lattice. The numbers indicate temperature. Note that the linear (algebraic) region is most prominent for $T = 0.44$ and fits to $75 \times 10^6 t^{-1.9}$.

### *3.1. Energy*

The study of energy relaxation for $\kappa > 0.5$ follows closely the procedure for $\kappa < 0.5$, with the only difference that the initial configuration is now the antiphase. For $\kappa = 0.60$, the energy relaxation depends on size predominantly at $T = 0.43$ and 0.44 (figure 8) and for $L = 700$, the energy difference $E(t) - E(\infty)$ shows an algebraic decay over an extended region of time at $T = 0.43$ and 0.44 (figure 9). Therefore, at $\kappa = 0.60$ we identify $T_c$ as $0.44 \pm 0.01$. The curves for $\kappa = 0.55$ are qualitatively similar to that for $\kappa = 0.60$, and $T_c$ could be identified as $0.37 \pm 0.01$. An alternative interpretation of the results could be that the floating phase would exist, if at all, between $T = 0.43$ and 0.44 (0.37 to 0.38) at $\kappa = 0.60$ (0.55). That the energy does not show any critical behaviour over an extended range of temperature, seems to indicate that the floating phase does not exist over an extended region.

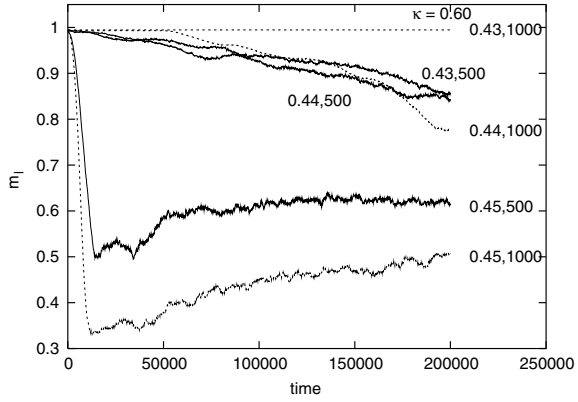


**Figure 10.** Relaxation of layer magnetization for $\kappa = 0.60$ at temperature $T$ for $L \times L$ square lattice. The numbers at the right margin indicate $T$ and $L$ values.

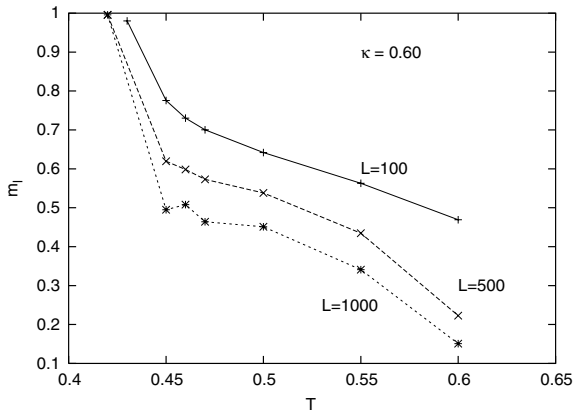


**Figure 11.** Equilibrium value of layer magnetization at $\kappa = 0.60$ as a function of temperature.

We mention that we could not perform the study of energy relaxation at $\kappa = 1$, since for this case reliable data need averaging over too many configurations.

The exponent for energy relaxation $\sigma'$ (see equation (5)) is found to be $1.7 \pm 0.1$ for $\kappa = 0.55$ and 0.60. In contrast to the findings for $\kappa < 0.5$, we observe no marked variation of $\sigma'$ with $\kappa$.

### *3.2. Layer magnetization*

The relaxation of layer magnetization ($m_l$) is qualitatively similar for $\kappa = 0.55$, 0.60 and 1.00. At $\kappa = 0.60$ the relaxation shows critical slowing down and finite size effect at $T = 0.44 \pm 0.01$ (figure 10), which is therefore the value of $T_2$. The equilibrium value of layer magnetization also shows a sharp fall (that becomes sharper as the system size increases) at this temperature, at $\kappa = 0.60$ (figure 11). For $\kappa = 0.55$ the value of $T_2$ can be estimated in a similar manner to be $0.37 \pm 0.01$. We could not observe the curve for equilibrium value of layer magnetization at $\kappa = 1$ because for this case one needs too long simulation to get the equilibrium value.

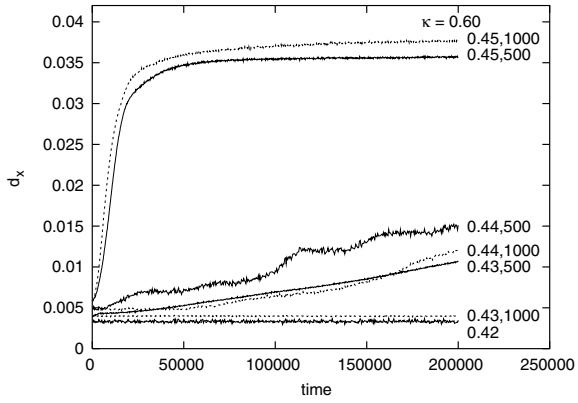


**Figure 12.** Relaxation of $d_x$ for $\kappa = 0.60$ at temperature $T$ for $L \times L$ square lattice. The numbers at the right margin indicate $T$ and $L$ values. For $T = 0.42$, the curves for $L = 500$ and 1000 coincide.

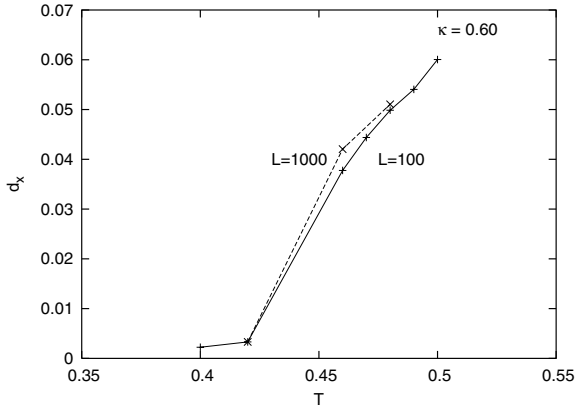


**Figure 13.** Equilibrium value of $d_x$ at $\kappa = 0.60$ as a function of temperature.

### *3.3. Length of domain walls parallel to the direction of frustration*

Like layer magnetization, this quantity ($d_x$) shows critical slowing down and finite size effect at $T = 0.44$ for $\kappa = 0.60$ (figure 12). The equilibrium value of $d_x$ shows a sharp rise at this temperature (figure 13), and this rise becomes sharper as the system size increases. Hence, the study of $d_x$ indicates that $T_c$ is $0.44 \pm 0.01$ for $\kappa = 0.60$. In the same manner, the value of $T_c$ is estimated to be $0.37 \pm 0.01$ for $\kappa = 0.55$ and $0.76 \pm 0.01$ for $\kappa = 1.00$.

### *3.4. Fraction of domains that have length 2*

A study of this quantity ($f_2$) leads to $T_c = 0.44 \pm 0.01$ for $\kappa = 0.60$, since size-dependent slowing down of the relaxation of $f_2$ is observed at this temperature (figure 14). Moreover, a sharp fall of the equilibrium value of $f_2$ is observed at this temperature and this fall becomes slightly sharper as the system size increases from 100 to 1000 (figure 15). In a similar manner,

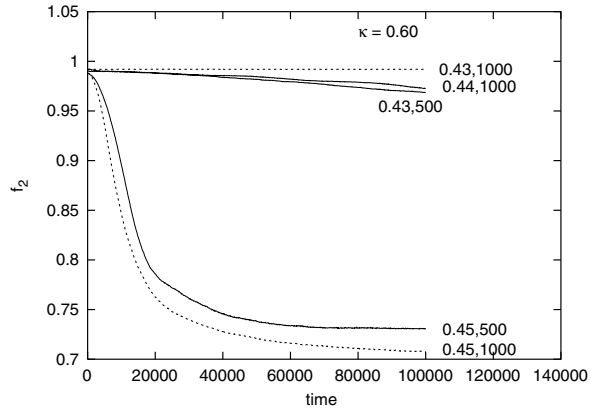


**Figure 14.** Relaxation of $f_2$ for $\kappa = 0.60$ at temperature $T$ for $L \times L$ square lattice. The numbers at the right margin indicate $T$ and $L$ values.

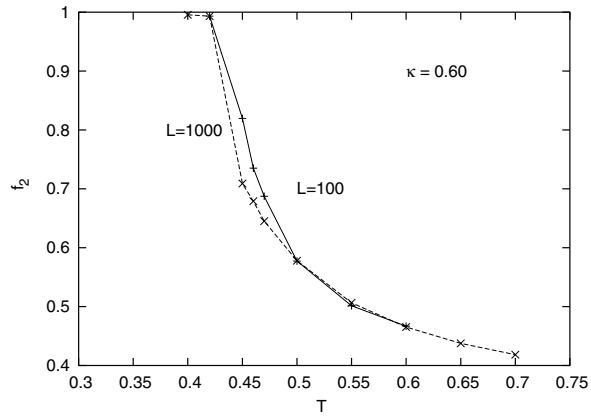


**Figure 15.** Equilibrium value of $f_2$ at $\kappa = 0.60$ as a function of temperature.

the critical temperature for $\kappa = 0.55$ and 1.00 is obtained as $0.37 \pm 0.01$ and $0.76 \pm 0.01$ respectively.

### *3.5. Fraction of domains that do not touch the boundary ($f_d$)*

We could not study the relaxation of this quantity since averaging over too many realizations is necessary for a reasonably smooth curve. Rather, we could measure the equilibrium value at temperatures where the relaxation was not prohibitively slow. It is found that for $\kappa = 0.60$, the critical temperature lies between 0.42 and 0.45, since a sudden change is observed in the equilibrium value of $f_d$ in this temperature range and that this change becomes more and more sudden as the lattice size increases (figure 16). Similar behaviour is also observed for $\kappa = 0.55$ between temperature 0.35 and 0.40. This study could not be done for $\kappa = 1.0$ because of computational limitation (one has to average over a good number of realizations to get reliable data). In spite of the computational difficulties for the study of $f_d$, it is clear that

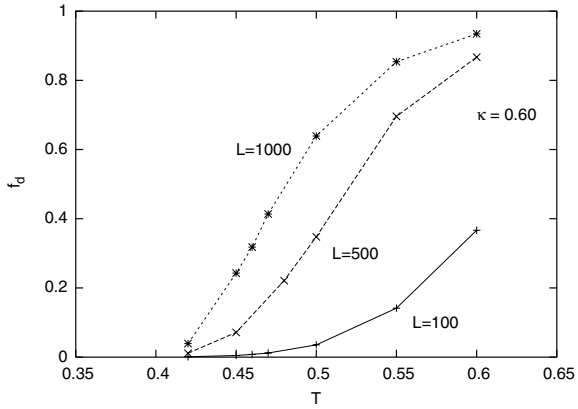


**Figure 16.** Equilibrium value of $f_d$ at $\kappa = 0.60$ as a function of temperature.

the study of this quantity excludes the possibility of a critical region with a width larger than 0.02 along the temperature axis.

## 4. Mapping to a quantum model

A quantum Ising model in the $d$ dimension is related to a classical Ising model in the $d + 1$ dimension by Suzuki–Trotter transformation [7, 9, 10] and this relation is the basic idea behind the quantum Monte Carlo algorithm. This transformation for the ANNNI model has been discussed in detail by Arizmendi [8] and can be summarized as follows. The quantum Ising Hamiltonian $\mathcal{H}_q$ for the one-dimensional transverse ANNNI model with $N$ sites is given by

$$\mathcal{H}_q = -J' \sum_{j=1}^{N} \left( s_j^z s_{j+1}^z - \kappa s_j^z s_{j+2}^z \right) - \Gamma \sum_{j=1}^{N} s_j^x. \tag{8}$$

The ground state for this model is equivalent to a classical Ising model in two dimension with Hamiltonian

$$\mathcal{H}_{cl} = -\sum_{x=1}^{N} \sum_{y=1}^{mn} J_q s_{x,y} [(s_{x+1,y} - \kappa s_{x+2,y}) + p s_{x,y+1}] \tag{9}$$

in the limit $(m \to \infty)$ and $(n \to \infty)$ at a temperature $T_q$ where

$$\frac{k_B T_q}{J_q} = \frac{m\Gamma}{J'} \tag{10}$$

($k_B$ is the Boltzmann constant) and

$$p = \frac{m\Gamma}{2J'} \log[\coth(1/m)]. \tag{11}$$

Obviously, the nearest-neighbour interaction in the $y$ direction is $p$ times the same in the $x$ direction and as $m \to \infty$ this ratio $p$ also tends to infinity.

As mentioned earlier, the Hamiltonian $\mathcal{H}_q$ of equation (8), describing a transverse ANNNI chain, has also been studied widely and numerical and (approximate) analytic studies [9, 11–13] had predicted the existence of floating phase over a wide region extending from $\kappa < 0.5$ to $\kappa > 0.5$ (figure 17). Why then this extensive presence of floating phase does not

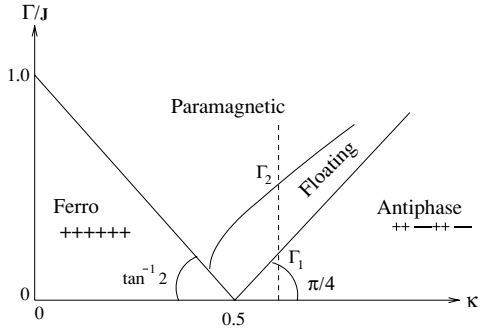


**Figure 17.** Schematic phase diagram for the transverse ANNNI model (with Hamiltonian $\mathcal{H}_q$ of equation (8)), after [13]

**Table 1.** Conclusions regarding the critical region from the study of various observables (sections 2 and 3 here). $T_0$ is the temperature (in units of $T_c^{(0)} = 0.44069$) at which there is a critical region of width $< 0.02$.

| $\kappa$ | $T_0$ |
|---|---|
| 0.45 | 0.404 |
| 0.55 | 0.37 |
| 0.60 | 0.44 |
| 1.0 | 0.76 |

occur in the phase diagram of figure 2? It seems that the explanation is the following. For the classical Hamiltonian $\mathcal{H}_{cl}$ of equation (9), the strength of nearest-neighbour interaction in the $Y$ direction is $p$ times stronger than that in the $X$ direction, thus stabilizing the order in the $Y$ direction. This raises both the upper critical temperature $T_2$ (at which the order in the $Y$ direction breaks down) and the the lower critical temperature $T_c$ (at which the order in the $X$ direction breaks down). Both the temperatures are raised by almost the same amount (thus the floating phase always has negligible width) but the amount of rise depends on the value of $p$. Now consider the quantum Hamiltonian $\mathcal{H}_q$. For a given $\kappa$ if the floating phase extends from $\Gamma_1$ to $\Gamma_2$ ($\Gamma_2 > \Gamma_1$, the difference $\Gamma_2 - \Gamma_1$ being appreciable), then the value of $p$ (say, $p_2$) corresponding to $\Gamma_2$ will be proportionately larger than the value of $p$ (say, $p_1$) corresponding to $\Gamma_1$ (see equation (11)). Although for every value of $p$, one has $T_c \approx T_2$, the common value of $T_c$ and $T_2$ at $p_2$ is appreciably larger than that at $p_1$. This shows that the *presence* of floating phase over a wide parameter region for the quantum model is consistent with the *absence* of the same for the classical model.

## 5. Conclusions

(1) For the 2D ANNNI model, diverging correlation length and algebraically decaying spin–spin correlation exist only along a 'line'. We present in table 1 the temperature $T_0$ such that within the temperature range $(T_0 - 0.01) < T < (T_0 + 0.01)$ lie both the upper critical temperature $T_2$ and the lower critical temperature $T_c$. We did not conduct the study at temperature intervals smaller than 0.01 except at $\kappa = 0.45$.

(2) The phase diagram is topologically different for the 2D ANNNI model and its Suzuki-Trotter counterpart, the 1D transverse ANNNI chain. This is in contradiction with

the fact that often a quantum model and its corresponding classical counterpart show topologically similar phase diagram and have the same critical indices at the transition point. Two examples of such behaviour are (i) the 2D Ising model and the 1D transverse Ising model with nearest-neighbour interaction ($\kappa = 0$) [20] and (ii) *XYZ* chain and the eight-vertex model [21].

## Acknowledgments

The work of one author (AKC) was supported by UGC fellowship. We also acknowledge the financial support from DST-FIST for computational facility.

## References

[1] Selke W 1988 *Phys. Rep.* **170** 213
Selke W 1992 *Phase Transitions and Critical Phenomena* vol 15, ed C Domb and J L Lebowitz (New York: Academic) pp 1–72
[2] Yeomans J 1988 *Solid State Physics* vol 41, ed H Ehrenrich and D Turnbull (New York: Academic) pp 151–200
[3] Liebmann R 1986 *Statistical Mechanics of Periodic Frustrated Ising Systems* (Berlin: Springer)
[4] Villain J and Bak P 1981 *J. Phys. (Paris)* **42** 657
[5] Shirahata T and Nakamura T 2001 *Phys. Rev.* B **65** 024402
[6] Derian R, Gendiar A and Nishino T 2006 *J. Phys. Soc. Japan* **75** 114001 (*Preprint* cond-mat/0605411)
[7] Suzuki M 1987 *Quantum Monte Carlo Methods* ed M Suzuki (Berlin: Springer)
[8] Arizmendi C M, Rizzo A H, Epele L N and Canal C A Garcia 1991 *Z. Phys.* B **83** 273
[9] Chakrabarti B K, Dutta A and Sen P 1996 *Quantum Ising Phases and Transitions in Transverse Ising Models* (Berlin: Springer)
[10] Chakrabarti B K and Das A 2005 *Quantum Annealing and Related Optimization Methods* ed B K Chakrabarti and A Das (Berlin: Springer) (*Preprint* cond-mat/0312611)
[11] Uimin G and Rieger H 1996 *Z. Phys.* B **101** 597
[12] Dutta A and Sen D 2003 *Phys. Rev.* B **67** 094435
[13] Chandra A K and Dasgupta S 2007 *Phys. Rev.* E **75** 021105 (*Preprint* cond-mat/0612144)
[14] Fisher M E 1976 *Phys. Rev.* B **13** 5039
Binder K and Heermann D W 2002 *Monte Carlo Simulations in Statistical Physics* 4th edn (Berlin: Springer) p 55
Landau D P and Binder K 2000 *A Guide to Monte Carlo Simulations in Statistical Physics* (Berlin: Springer) chapters 2 and 4
[15] Sato A and Matsubara F 1999 *Phys. Rev.* B **60** 10316
[16] Rutenberg A D and Bray A J 1995 *Phys. Rev.* B **51** 5499
[17] Wansleben S and Landau D P 1991 *Phys. Rev.* B **43** 6006
[18] Ma S K 1976 *Modern Theory of Critical Phenomena* (New York: Benjamin)
Fisher M E and Racz Z 1976 *Phys. Rev.* B **13** 5039
[19] Janssen H K, Schaub B and Schmittmann B 1989 *Z. Phys.* B **73** 539
Zheng B 1998 *Int. J. Mod. Phys.* **12** 1419
Sen P and Dasgupta S 2002 *J. Phys. A: Math. Gen.* **35** 2755
[20] Mattis D C 1985 *The Theory of Magnetism* vol II (Berlin, Heidelberg: Springer) section 3.6
[21] Baxter R J 1982 *Exactly Solved Models in Statistical Mechanics* (London: Academic) p 266